Ecological Indicators 127 (2021) 107485

Contents lists available at ScienceDirect

Ecological Indicators

journal homepage: www.elsevier.com/locate/ecolind

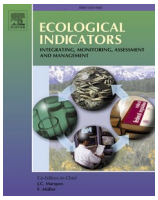

Mapping and assessment of wetland conditions by using remote sensing images and POI data

Zhaohui Yang *, Junwu Bai, Weiwei Zhang

School of Environmental Science & Engineering, Suzhou University of Science and Technology, 99 Xuefu Road, Suzhou 215009, Jiangsu, China

ARTICLE INFO

Keywords:
Wetland
Remote sensing
Knowledge-based raster mapping (KBRM)
Point of interest (POI)
Mapping and assessment

ABSTRACT

Wetlands are one of the most valuable natural resources on earth and play an important role in preserving biodiversity. However, due to economic development and human disturbances, many wetlands across the world have deteriorated and disappeared over the past several decades. By using remote sensing images and point of interest (POI) data, we proposed a knowledge-based raster mapping (KBRM)-based framework and implemented it in the assessment of wetland ecological conditions in Suzhou, China. Density maps of waterbodies, vegetation covers, imperviousness, roads, and POI values were derived and used as five ecological indicators that can represent the ecological conditions of wetlands. The KBRM approach was used to integrate these indicators into an overall rating and map wetland ecological conditions efficiently. Thus, spatial variations in wetland ecological conditions can be distinguished and represented in detail. Cross validation was conducted with water quality data at 15 field sampling sites. The validation results demonstrated that the overall wetland condition scores generated by our approach and the water quality index (WQI) values calculated from water quality data were strongly correlated. These findings confirm that our framework could be used to effectively map and evaluate spatial variations in wetland ecological conditions and provide more support for policy-making in wetland protection and management

1. Introduction

Wetlands are one of the most valuable natural resources in the world, as they provide important habitats for a wide range of animal and plant species and serve a variety of natural, economic, social, and cultural functions (Mwita et al., 2013). However, due to economic development and human disturbances, many wetlands across the world have undergone a variety of stress-inducing alterations, including hydrologic modification, land-use change alteration, pollutant runoff contamination, eutrophication, and fragmentation, which has resulted in heavy impacts on wetland conditions. Wetland conditions concern the health or quality of wetlands and refer to the extent to which a site departs from full ecological integrity (Fennessy et al., 2004). Ecological integrity is the sum of physical, chemical, and biological integrity characteristics, which indicates correspondence with the original ideal wetland condition (Fernandez et al., 2019). Wetland conditions, which are largely dependent on disturbances within and outside wetlands and their landscape types, are related to conservation and restoration activities and mitigation planning and decisions at sites or landscape scales. Thus, scientists and practitioners involved in wetland monitoring, construction, protection, restoration, and management need appropriate assessment methods to evaluate the quality, performance, and relative success of their work (Mollard et al., 2013).

In the past several decades, a wide variety of assessment methods for wetland conditions have been developed and implemented, ranging from rapid qualitative assessment methods to intensive quantitative methods (Langan et al., 2019). Among them, a three-tiered approach is commonly used to assess wetland conditions by the US Environmental Protection Agency (EPA, 2006). Level 1 wetland assessments are landscape-level methods that rely primarily on remote sensing and geographic information system (GIS) technologies. It can be used to rapidly acquire landscape-scale information about wetland conditions without the need for expensive and time-consuming field-based visits. Level 2 wetland assessments contain a medium intensity evaluation that requires rapid fieldwork and quantifies wetland conditions using relatively simple semiquantitative or qualitative field-based indicators (Fennessy et al., 2007). Level 3 wetland assessments involve the most intensive evaluation methods and require detailed field measurements

* Corresponding author.
E-mail addresses: zhaohuiyang@mail.usts.edu.cn (Z. Yang), zhangweiwei@usts.edu.cn (W. Zhang).

https://doi.org/10.1016/j.ecolind.2021.107485
Received 27 October 2020; Received in revised form 31 January 2021; Accepted 31 January 2021
Available online 25 April 2021

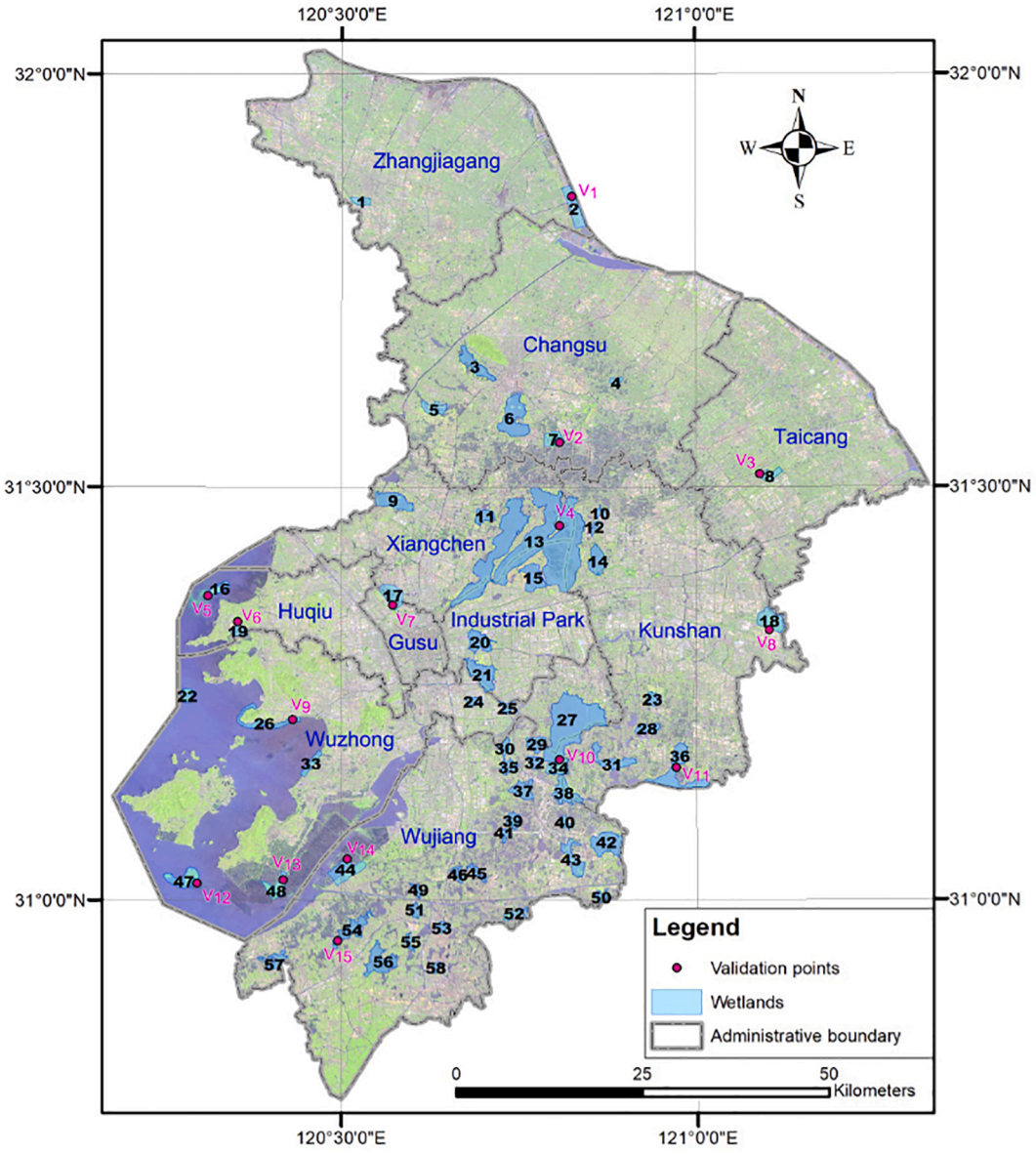

Fig. 1. Locations of 58 wetlands assessed in the study area. The numbers correspond to the descriptions of Table A1.

(Stryszowska-Hill et al., 2019).

The choice of a specific level of assessment depends on different factors, such as budget, availability of relevant data at appropriate scales, technical capacity, and wetland accessibility (Tiner, 2018). Level 2 and Level 3 assessments can obtain more representative and detailed results than Level 1 assessments. However, fieldwork and lab analyses make them expensive in terms of cost, labor and time. Therefore, they are often not affordable for large areas or inaccessible sites, especially those in developing countries (Cools et al., 2013). Conversely, Level 1 assessments, which are based on the analysis of information from maps and remotely sensed imagery coupled with a basic understanding of wetlands, are designed to evaluate wetland conditions for large geographic areas with low costs and a high regional transferability (Stryszowska-Hill et al., 2019).

The development of GIS and remote sensing technologies brings about significant improvements and new possibilities for Level 1 assessments. The supply of high-quality environmental data expands considerably when using these spatial information technologies (Yang et al., 2016a). Various landscape-level indicators, such as land-cover type, landscape fragmentation, slope gradient, wetland area, and aquatic connectivity, have been adopted to represent wetland conditions (Brooks et al., 2004; Mamoun et al., 2013; Weller et al., 2007). Based on these indicators, a variety of methods have been applied to infer and assess wetland conditions. Ausseil et al. (2007) used a weighted average of the scores of individual indicators to rank wetland conditions in New Zealand. Brown and Vivas (2005) proposed a landscape development intensity index (LDI) derived from emergy use per unit and land use data. It has been applied to wetland condition and habitat assessments in a few countries (Lane and Brown, 2007; Mack, 2006; Wang et al., 2020). Some scholars have designed a remote sensing-based ecological index (RSEI), which was formulated by integrating four indicators via principal component analysis (PCA) rather than a traditional weighted sum method (Xu et al., 2018; Jing et al., 2020). Sun et al. (2016) assessed wetland ecosystem health using the pressure-state-response (PSR) model by synthesizing remote sensing and statistical data. Yang et al. (2017) used the random forest method to select features from landscape indicators and realized wetland landscape assessment with a support vector machine.

Additionally, there are multiple sources of social and economic indicators (e.g., population density and welfare index) integrated into

Level 1 assessments (Chen et al., 2019). Among them, point of interest (POI) data, which are recorded for three attributes (type, name, and geoposition), have been widely applied to understand urban environments from the human activities perspective (Liu et al., 2017). Given the availability of the location and related attributes of POIs, there has been steadily growing interest in studying a variety of research challenges in identifying, monitoring and analyzing POIs. In particular, POIs have a broad range of applications, including geomarketing, event management, and urban planning (Tran et al., 2021). Additionally, spatial patterns or distribution densities derived from POI data can represent human disturbances to urban and wetland regions (Chen et al., 2018). However, they rarely applied POI data to assess wetland conditions.

The available data on the Suzhou wetlands are far from sufficient for governmental use in generating a concrete plan for protection and restoration. It is impossible for a Level 2 or Level 3 assessment to cover all wetlands with the current limited field data. Therefore, our goal is to develop a responsive, practical, cost-effective, and ecologically meaningful framework to assess the conditions of wetlands in Suzhou, China.

The process of selecting indicators is challenging because ecological conditions can be assessed at a variety of locations, sizes, types and scales. Indicators should provide reliable, cost-effective, and ecological representations of wetland conditions (Faber-Langendoen et al., 2019). Deriving appropriate indicators and implementing reasonable assessments are challenging problems. Based on previous studies, other published literature and data availability, five indicators (density maps of waterbodies, vegetation covers, imperviousness, roads, and POI) were derived and quantified based on remote sensing images and POI data. Water, vegetation, and imperviousness are three main biophysical components of wetland ecosystems (Xu et al., 2018). Water has a major influence on the habitats of species living in wetlands (Ausseil et al., 2007). Vegetation plays an important role in nutrient cycles and productivity as well as in reducing the effects of erosion and flooding (Mitsch and Gosselink, 2000). Imperviousness is used to identify anthropogenic features that affect wetland environments (Liu et al., 2019a). Roads are commonly identified as having strong negative effects on wildlife and their habitats in wetlands (Fernandez et al., 2019). These five indicators are closely related to landscape patterns and human activities, which can be directly perceived by people and are used to evaluate ecological conditions.

Our overall objective is to aggregate ecological indicators into an overall rating and develop an easily accessible framework to guide and refine the assessment of wetland conditions. Specifically, in this study, we (1) derived and integrated appropriate ecological indicators from remote sensing images and POI data; (2) identified the characteristics of spatial differentiation in wetlands; and (3) validated the effectiveness of the assessment results obtained by our method. The results could help relevant wetland managers develop scientific policies for wetland condition mapping and assessment and promote efficient protection and sustainable utilization of wetland resources.

2. Study area and dataset

2.1. Study area

Suzhou is located in the southeastern Jiangsu Province and central Yangtze River Delta, China, within a range of 119°55′-121°20′E and 30°47′–32°02′N. It contains six districts (i.e., Gusu, Huqiu, Industrial Park, Xiangchen, Wuzhong, and Wujiang) and four satellite cities (namely, Kunshan, Changshu, Taicang, and Zhangjiagang) (Xiao et al., 2018). As a major tourism destination, Suzhou is renowned for its historic gardens and cultural heritages. Sometimes referred to as the “Water City” and “Land of Fish and Rice”, Suzhou is rich in wetland resources and famous for its dense river network and lake system as well as its man-made canals. Over the past several decades, Suzhou has experienced rapid economic growth that has caused resource overexploitation, environmental pollution, and ecosystem degradation (Long et al., 2015), which have imposed negative impacts on Suzhou’s wetland system, such as continuous deterioration, area shrinkage, bird and fish population reduction, and biological diversity diminution (Suzhou Municipal Agricultural Committee, 2010). To protect and restore degraded wetlands, the municipal government of Suzhou conducted a preliminary survey of wetlands in 2009, which mainly included lacustrine wetlands. From 2014, the municipal government of Suzhou began to build several monitoring sites that were representative of the water quality and aquatic ecology of the wetlands. These monitoring sites were selected to be located across various wetlands in Suzhou. However, field data collected from these monitoring sites are still scarce. The paucity of field data, mainly due to the expensive and slow nature of field sampling, has hindered the assessment and management of wetlands (Salari et al., 2014).

Our specific study area is the administrative region of Suzhou, with an area of 7260 km^2. It includes all six districts and four satellite cities. In the study area, 58 wetlands or wetland parks, which have been identified as municipal-level important wetlands by the municipal government of Suzhou (http://ylj.suzhou.gov.cn/szsylj/sdgk/wztt.shtml), are included with a total area of 408.5 km^2 (Fig. 1). Among them, the largest is the Yangchenghu Wetland (13), with an area of 109.843 km^2. The smallest one is the Manlihu Wetland (12), which occupies an area of only 1.136 km^2.

Table 1
Datasets used in this study and their formats, sources and purposes.

Dataset	Format	Spatial resolution/ Source scale	Source	Purpose
Landsat 8 OLI images (Path: 119, Row: 38, Path: 119, Row: 39)	Raster	30 *m*	USGS website http://glovis.usgs.gov	Density map of waterbodies Density map of vegetation covers Density map of imperviousness
Road network	Polyline shape	–	OpenStreetMap (OSM) https://www.openstreetmap.org	Density map of roads
POI	Points shape	–	Baidu Map Company, Chinah ttp://map.baidu.com	Density map of POI values
Wetlands Inventory	Polyline shape	1:10,000	Wetland Protection Station of Suzhou	Boundary of 58 wetlands
Administrative boundaries	Polyline shape	1:10,000	Wetland Protection Station of Suzhou	Boundary of districts in Suzhou

2.2. Data collection

Table 1 describes the five types of data that were acquired for this study. Landsat 8 OLI images taken on 2017–5-27 were retrieved from the US Geological Survey (USGS) website (https://glovis.usgs.gov), with path/row of 119/38 and 119/39 and a spatial resolution of 30 m. The wetland inventory and administrative boundaries in vector format were obtained from the Wetland Protection Station of Suzhou. Road network data were collected from OpenStreetMap (OSM) (https://www.openstreetmap.org). As the pioneer Volunteer Geographic Information (VGI) project, OSM data are freely available with relatively high positional accuracy in urban regions. POI data were retrieved in 2017 from the Baidu Map Company (http://map.baidu.com), one of the most

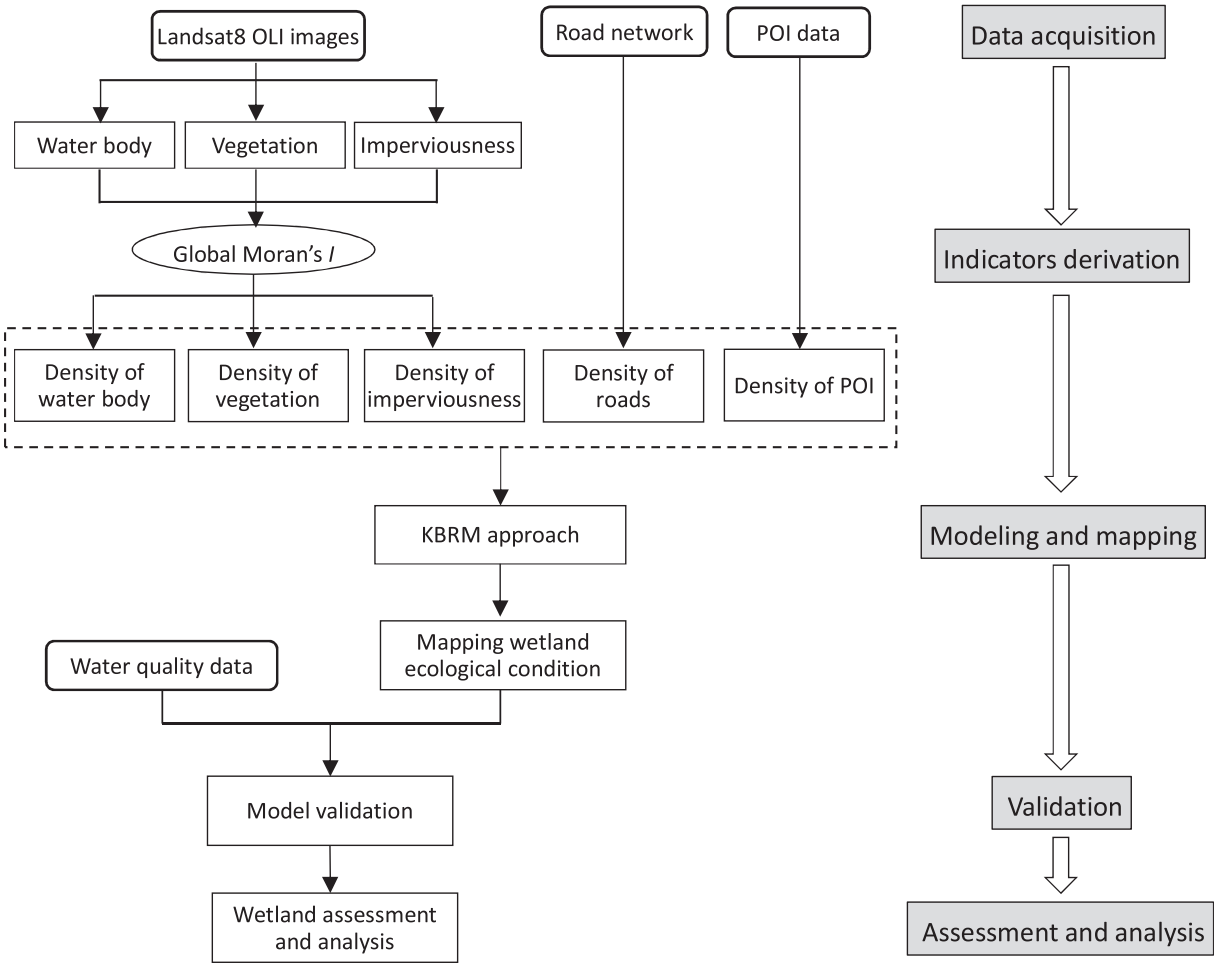

Fig. 2. Flowchart for this study. Steps of indicator derivation, integration, mapping, validation, and assessment are included in the workflow.

popular map services in China. A total of 401,646 records of POI data, which were classified into 20 categories by the Baidu predefined classification system, were obtained within the study area.

ArcGIS10.3 and ENVI5.3 + IDL8.5 were used to process the raw data, calculate ecological indicators, and generate an assessment framework. Radiometric and atmospheric corrections were performed to convert the digital number (DN) of the raw Landsat 8 OLI images to the reflectivity of the sensor.

3. Methods

We built a detailed workflow for this study (Fig. 2). This workflow included three major components. First, five indicators (i.e., density of waterbodies, vegetation covers, imperviousness, roads, and POI) were extracted and derived from the raw data. Second, based on the KBRM approach, five indicators were integrated into an overall score map that represented wetland conditions. Third, we validated our method by using water quality data and performed wetland condition assessments.

3.1. Derivation of ecological indicators

To understand the condition of wetlands in Suzhou, a total of five indicators were extracted and derived. First, three major features were retrieved from Landsat 8 OLI images, including open water bodies (rivers and lakes), vegetation covers and imperviousness. Road network and POI data were acquired from open public data sources. Then, density maps of waterbodies, vegetation covers, imperviousness, roads, and POI values were processed and derived as ecological indicators.

3.1.1. Waterbody

For a lacustrine wetland, open water bodies have a determinant influence on the habitats of those species living in wetlands (Ausseil et al., 2007). The waterbody has a stronger absorbability in the SWIR band than in the NIR band, and the built-up class has a greater radiation in the SWIR band than in the NIR band. Based on this finding, an MNDWI index was proposed to extract the waterbody (Xu, 2006).

$$\mathrm{MNDWI} = \frac{\mathrm{GREEN} - \mathrm{SWIR}}{\mathrm{GREEN} + \mathrm{SWIR}} \quad (1)$$

where GREEN and SWIR are the TOA reflectance of GREEN and SWIR bands in Landsat 8 OLI images.

The original values of MNDWI range from −1.0 to 1.0. Based on visual interpretation, we only used the cells with values > 0.73 to represent the waterbody area. The higher the MNDWI value is, the more intensive the waterbody.

3.1.2. Vegetation

Wetland vegetation can reduce water velocity and contribute to impurity sedimentation and contaminant elimination. Additionally, it can provide habitats for birds and other animals (Pettorelli et al., 2011). Spectral vegetation indexes are most often used to estimate vegetation canopies from satellite images. The most commonly used index is the normalized difference vegetation index (NDVI) (Tucker et al., 1985). However, NDVI has been shown to be very sensitive to soil optical properties under incomplete vegetation cover conditions, which often occur in urban regions. Therefore, we calculated the soil-adjusted vegetation index (SAVI), which uses a soil adjustment factor L to

Table 2
Seventeen categories of POIs and the counts for each category. LDI coefficients were used as the weights for each category.

ID	Category	Counts	Classes used by Chen and Lin (2013)	LDI coefficients
1	Gasoline station	705	Gasoline station	8.07
2	Auto service	8162	House for residence and business	8.66
3	Restaurant	41,079	Service industry	9.18
4	Retail	142,490	Retail and wholesale stores	8.00
5	Entertainment	8280	Amusement place	6.92
6	Hospital and clinic	8057	Hospital and health care facility	8.07
7	Hotel	5298	House for residence and business	8.66
8	Park	2704	Park (green yard)	1.83
9	Residential community	13,530	Residential house	6.79
10	Government agency	20,998	Governmental Building	8.07
11	Education facility	7713	Elementary school/ middle school/other school	8.07
12	Public bike and park lots	15,630	Road facility	8.28
13	Bank and ATM facility	6981	House for residence and business	8.66
14	Company	86,098	Manufacturing building	8.07
15	Toll station and road facility	466	Road facility	8.28
16	Transport facility	29,614	Road facility	8.28
17	Public toilet and kiosk	3841	House for residence and other uses	8.66

account for soil background variations and is more useful for identifying vegetated areas in urban regions (Huete, 1988). The SAVI is expressed as follows:

$$\mathrm{SAVI} = (\mathrm{NIR} - \mathrm{RED})(1 + L)/(\mathrm{NIR} + \mathrm{RED} + \mathrm{L})$$

where RED and NIR denote a red band and a near-infrared band of Landsat 8 OLI images, respectively; L is 0.5 for urban areas.

The original values of the SAVI range from −1.5 to 1.5. According to experts' field experience and on-screen visual interpretation, we only used the cells with values > 0.6 to represent the vegetation area. The higher the SAVI value is, the denser the vegetation cover.

3.1.3. Imperviousness

Impervious surfaces, such as house roofs, parking lots and paved roads, refer to land cover types that prevent water filtration into soil (Arnold and Gibbons, 1996). Impervious surfaces not only indicate the process of urbanization but also describe anthropogenic features that affect the relevant environment. We extracted the imperviousness and used it to represent the influence of built-up areas on wetlands. Following Xu (2008), we calculated a built-up index (IBI) and extracted the imperviousness.

$$IBI = \frac{2\mathrm{SWIR}_1/(\mathrm{SWIR}_1 + \mathrm{NIR}) - [\mathrm{NIR}/(\mathrm{NIR} + \mathrm{RED}) + \mathrm{GREEN}/(\mathrm{GREEN} + \mathrm{SWIR}_1)]}{2\mathrm{SWIR}_1/(\mathrm{SWIR}_1 + \mathrm{NIR}) + [\mathrm{NIR}/(\mathrm{NIR} + \mathrm{RED}) + \mathrm{GREEN}/(\mathrm{GREEN} + \mathrm{SWIR}_1)]} \quad (3)$$

where SWIR_1, NIR, RED and GREEN are the middle infrared band, near infrared band, red band and green band of Landsat 8 OLI images, respectively.

The original values of the IBI range from −1.0 to 1.0. Similarly, by combining experts' field experience with on-screen visual interpretation, we designated those areas whose IBI values were greater than −0.2 as impervious surfaces.

3.1.4. Road network

Roads are commonly recognized as exerting cumulative negative effects on wildlife and their habitats. Road density is a common metric used to measure these effects (Weller et al., 2007). Some roads have been identified from remote sensing images using an indicator of imperviousness; however, because of the limitation of the low spatial resolution of these images, many roads still cannot be extracted as imperviousness. Therefore, we also derived road density indicator from road networks. To avoid double counting, roads should be subtracted from impervious surfaces before calculating the road density (Fernandez et al., 2019). In this paper, we used the extraction tool in ArcGIS10.3 to remove the parts of roads within impervious surfaces.

Road network data were downloaded from OSM and classified into several levels (e.g., highway, primary, secondary, tertiary, cycleway, footway, and pedestrian) based on their relative importance. We integrated them into three classes (namely, primary, secondary, and others). Based on the ratios of the average traffic flow between them, 5, 3 and 1 were assigned as their weights.

3.1.5. POI

POI data, which are provided voluntarily by individuals, often include transport facilities, educational institutes, government agencies, commercial services, residential buildings, companies, etc. Each point of POI contains the functional and locational properties of a linked site. POI data can link geographic locations to specific places, particular features, and other site-based information. Therefore, they are fundamental for their use as an important indicator of human disturbance, which is often used to generate urban land use and social functional mapping (Chen et al., 2018; Hu et al., 2016).

The initial 20 classes of POIs captured from the Baidu maps were aggregated into 17 general categories. Table 2 presents the 17 categories of POIs and the counts for each category. The quality of the POI data was verified by checking 510 randomly sampled sites manually (i.e., 30 sites for each category, which are evenly distributed in the study area). The resulting accuracy level was 95%. Although spurious data may be included, the overall distribution pattern can be accurately represented by using a large number of sites.

Considering that different categories are linked to different human activities and may have different impacts on wetland conditions, we implemented the idea of the landscape development intensity (LDI) index developed by Brown and Vivas (2005). The LDI is intended for use as an index of the human disturbance gradient because the intensity of human-dominated land uses may affect the biodiversity of adjacent wetlands through direct and/or indirect impacts.

The metric for quantifying human activities was emergy use per unit area per time. It is measured as the solar emergy joule sej per ha per year and is calculated from nonrenewable energy sources, including electricity, fuel, fertilizer, pesticide, and water applications (Brown and Vivas, 2005). The calculated emergy values are normalized as LDI coefficients and range from 1 to 10 calculated as the normalized natural log of energy per area per time. The higher the LDI coefficient is, the greater the degree of human disturbance. Here, we assigned the weights for individual POI categories (see Table 2) based on the LDI coefficients used by Brown and Vivas (2005) and Chen and Lin (2013).

3.1.6. Spatial autocorrelation analysis

Characteristics of the spatial distribution are commonly referred to as the spatial autocorrelation, which is measured by Moran's index (*I*) and Geary's index (Upton and Fingleton, 1985). Spatial autocorrelation can be divided into global spatial autocorrelation and local spatial autocorrelation, which can reveal the correlation of the attribute values between the spatial reference unit and its adjacent space unit.

The global Moran's *I* index was used to analyze the global spatial correlation of individual indicators in the study area and can be calculated using the following equation (Moran, 1948):

$$I(d)\left[\frac{1}{W(d)}\right] = \frac{\sum_{i=1}^{n}\sum_{\substack{j=1\\ j\neq i}}^{n} w_{ij}(d)(x_i-\bar{x})(x_j-\bar{x})}{\frac{1}{n}\sqrt{\sum_{i=1}^{n}(x_i-\bar{x})^2}} \quad (4)$$

where $w_{ij}(d)$ stands for the spatial contiguity weights matrix that indicates whether a pair of sampling locations are in distance class d; x_i and x_j are the values of variable x at sampling locations i and j; $W(d)$ is the sum of $w_{ij}(d)$, which is the number of pairs of sampling locations per distance class; and $\bar{x}$ is the mean of the corresponding attributes.

Global Moran's *I* index values range from −1 to 1. Values > 0 indicate that the space is in positive autocorrelation. The greater the number is, the stronger the autocorrelation of the spatial distribution. Conversely, values < 0 indicate that the space has a negative autocorrelation. We calculated the global Moran's *I* indexes for waterbodies, vegetated areas and imperviousness with different distance thresholds. From them, distance thresholds were set as appropriate bandwidths of individual indicators according to the decreasing trend of global Moran's *I* indexes.

Local spatial correlation is also known as the local indicator of spatial association (LISA), which can reveal local variation between the local spatial reference unit and its adjacent space unit. Local spatial correlation analysis mainly involves the local Moran's I_i, which can be estimated as follows:

$$I_i(d) = \frac{(x_i-\bar{x})}{\frac{1}{n}\sum_{i=1}^{n}(x_i-\bar{x})^2}\sum_{\substack{j=1\\ j\neq i}}^{n} w_{ij}(d)(x_i-\bar{x}) \quad (5)$$

where $w_{ij}(d)$ is the spatial contiguity weights matrix given a local neighborhood search of radius d; the weights matrix can be actual weights (e.g., inverse distance weighting function) to emphasize the local neighborhood effect on local spatial pattern; x_i is the values of variable × at sampling location i; and $\bar{x}$ is the mean of the corresponding attributes.

A positive value for local Moran's I_i indicates that a feature has neighboring features with similarly high or low attribute values. A negative value for local Moran's I_i indicates that a feature has neighboring features with nonsimilar values. In this study, we used local Moran's I_i to analyze the local spatial variation in wetland conditions.

3.1.7. Kernel density estimation mapping

To quantify the impacts of individual indicators on wetland conditions, we calculated the density of waterbodies, vegetation covers, imperviousness, roads and POI values using the kernel density estimation method (KDE) (Silverman, 1986). KDE can be used to generate the density of features in a neighborhood around those features. In the density map of features, the density value at each cell reveals the influence received by a given location from such indicators. This density value takes into account both the distance (the closer a feature point is to the given location, the more influence the location receives from that feature point) and counts of the surrounding points (the more points near the given location there are, the more influence the location receives).

The optimal distances, estimated by global Moran's *I* indexes, were used as appropriate bandwidths in the KDE algorithm. Specifically, for POI, classes (LDI coefficients) were used as the population field when generating a density map with KDE.

3.2. Knowledge-based raster mapping (KBRM) approach

We derived five ecological indicators, namely, the density of waterbodies, vegetation covers, imperviousness, roads, and POI values. To integrate individual indicators into an overall score that can depict wetland conditions, we generated a knowledge-based raster mapping (KBRM) approach based on the wetland-environment model (Yang et al., 2016a). The model was used to make inferences about wetland conditions based on landscape-level data rather than directly relying on fieldwork. It consists of two steps: standardizing each ecological indicator and aggregating ecological indicators into the output overall score. Borrowed idea from Shi et al. (Shi et al., 2004, 2009), the model can be expressed as follows:

$$W_{ij} = P_{a=1}^{N}(E_{ij,a}) \quad (6)$$

$$E_{ij,a} = \begin{cases} V_1, if Z_{ij,a} < V_1 \\ Z_{ij,a}, if V_1 \le Z_{ij,a} \le V_2 \\ V_2, if Z_{ij,a} > V_2 \end{cases} \quad (7)$$

where (i,j) is the location of the processed cell; W_{ij} is an overall score of wetland condition at location (i,j), ranging from 0 (worst) to 1 (best); $E_{ij,a}$ and $Z_{ij,a}$ are the normalized and original values of indicator a *at* (i,j), respectively; V_1 and V_2 are the lower and upper thresholds of the reasonable indicator value; and N is the total number of ecological indicators.

For V_1 and V_2, the original value of each indicator follows a normal distribution, so we constructed a confidence interval with a 98% confidence level. The upper and lower bounds of the confidence interval were used as thresholds V_1 and V_2. Thus, some extreme values, those lower than the lower threshold V_1 or greater than the upper threshold V_2, can be excluded as outlier values. For E, we adopted a normalized function to standardize individual indicators ranging from 0 to 1. Additionally, assuming that waterbodies and vegetation have positive impacts on wetland conditions and imperviousness, roads and POI have negative impacts on wetland conditions, we conformed that the impacts of indicators on wetland conditions have a positive relationship by inverting values of imperviousness, roads and POI. For P, we used the weighted sum method to generate the final overall score for each cell location.

The analytic hierarchy process (AHP) method (Saaty, 1980; Goepel, 2013) was used to derive experts' knowledge and determine the appropriate weights of individual indicators. The AHP is a structured process that organizes and analyzes complex decisions based on mathematical functions. It eases the consideration of complex relationships among multiple indicators by providing only simple pairwise comparisons from experts and then derives weight for each indicator through calculation over the score matrix established by the comparisons. Some scholars have introduced AHP into wetland assessments to comprehensively evaluate wetland conditions (Chen et al., 2019).

Five experts from the Wetland Protection Station of Suzhou, who are very familiar with wetlands in Suzhou, have worked on determining the weights of indicators by using AHP. First, they performed a pairwise comparison matrix for five indicators with paired relative importance ranks. Second, the importance ranking was calculated based on the filled comparison matrix, and an eigenvector was obtained by the square root method, which represented the order of importance of ecological indicators. Finally, to check the consistency of the experts' pairwise scores, we calculated the consistency ratio and verified that it was less than or equal to 10%; otherwise, the pairwise comparison values were recalculated to improve the indicators' weighted consistency. Thus, the final weight of each indicator was the average of contributions from individual experts. All final weights were then normalized to sum to 1, which were 0.23, 0.18, 0.11, 0.13, and 0.35 for the waterbody,

vegetation, imperviousness, road, and POI indicators, respectively.

3.3. Correlation between KBRM output and ecological indicators

To obtain dominant indicators and examine the representation of wetland conditions generated by our method, the correlation between the KBRM output and the five indicators was analyzed. Considering that a bivariate normal distribution exists for the individual indicators, we calculated Pearson's correlation coefficient and used it to measure the degree of correlation between the KBRM output and the five indicators (Choi et al., 2010).

3.4. Wetland assessment

To better understand the representation of wetland conditions, the overall score map was divided into five levels, representing bad, poor, moderate, good, and excellent. At present, in the traditional method of grading assessment results, the thresholds are determined in terms of the maximum, minimum, average and standard deviation or equal interval division of the results. They are normally determined subjectively with some uncertainties (Feng et al., 2020). In this paper, we employed the natural breaks (Jenks) algorithm to generate the gradation of five levels. The natural breaks (Jenks) algorithm seeks to reduce the variance within classes while maximizing the deviation from the means between classes (Jenks, 1967). Because of its high aggregated distribution and low diversity, it can reflect the spatial distribution of and difference in wetland conditions and has a better performance than most of the other methods (Liu et al., 2019b).

To measure numerical variations in individual wetlands, the average and standard deviation (std) of all cells within each wetland from the overall score map were calculated. We used the average value to represent the entire ecological condition of each wetland. We also used the std values to represent the interior variation of a wetland.

To better understand the spatial distribution characteristics of wetland ecological conditions, a 600 m × 600 m grid was generated to resample the overall output map of the study area, and the local spatial correlation pattern was analyzed by using a local Moran's I_i cluster map. Four types of significant autocorrelations could be found. High values surrounded by high neighboring values were designated as high-high (HH), low values surrounded by low neighboring values were designated as low-low (LL), low values surrounded by high neighboring values were designated as low–high (LH), and high values surrounded by low neighboring values were designated as high-low (HL).

3.5. Validation

To evaluate the quality of wetland assessments derived from our method, we obtained water quality data from the Wetland Protection Station of Suzhou and used them to validate our method. These water quality data were collected at 15 sampling sites, most of which are located across various wetlands in Suzhou according to their accessibility and representativeness. These sampling sites are representative of the water quality and aquatic ecology of wetlands in Suzhou (Zhu et al., 2019).

The water quality samples were collected every two months in 2018 and preserved as outlined in the relevant guidelines (Wilson and Bayley, 2012). These samples were analyzed for 13 parameters of water quality, including water temperature (T), dissolved oxygen (DO), chemical oxygen demand (COD), total nitrogen (TN), nitrate nitrogen ($NO3^{-}$-N), total phosphorus (TP), turbidity, suspended matter (TSS), pH, chlorophyll-a (Chl-a), and total organic carbon (TOC). Because the impact of nutrients on the wetland environment cannot be ignored, we finally used DO, T, TN, TOC, and TSS as the main parameters of water quality.

The water quality index (WQI) was used to generate the overall outcome by integrating different parameters (Dobbie and Dail, 2013). The WQI is a common tool used for the quantitative assessment of water quality (Fox, 2014). It provides a summary of the entire water environment, which reflects the environmental characteristics of the study area. Using the WQI is easy for the public and policy makers to understand the complex conditions of an aquatic environment.

The most common weighted aggregation method of WQI normally includes steps of selecting parameters, calculating subindexes, assigning weights and generating the WQI (Yan et al., 2015).

(1) Selecting parameters

In this paper, DO, T, TN, TOC, and TSS were selected as the main parameters of water quality. According to the Surface Water Environment Quality Standard of China, water quality is divided into five categories, which correspond to the criterion set of {Excellent, Good, Fair, Poor, Bad} (Chinese Environmental Protection Agency, 2002). Related to this criterion set, each indicator has standard guideline values for each of the five categories.

(2) Calculating subindexes

After five water quality parameters have been selected, parameters with different units and dimensions can be converted into subindexes with a common scale, which are frequently within the range of 0–100 (Srebotnjak et al., 2012). In this paper, a simple linear interpolation function was used to calculate the subindexes (Uddin et al. 2021), which can be stretched from 0 to 100. A larger value of the subindex indicates a better water quality.

$$S_i = S_1 - \left[\left(S_1 - S_2 \right) \left(\frac{X_i - X_1}{X_2 - X_1} \right) \right] \tag{8}$$

$$S_i = S_1 - \left[\left(S_1 - S_2 \right) \left(\frac{X_1 - X_i}{X_1 - X_2} \right) \right] \tag{9}$$

where S_i is the subindex value for parameter i calculated for the observation value X_i; X_1 and X_2 are the maximum and minimum standard guideline values for parameter i; and S_1 and S_2 are the maximum and minimum subindex values of X_1 and X_2 for parameter i. When the value of the observation parameter was higher than the upper guideline value, Eq. (8) was used. Otherwise, Eq. (9) was implemented.

(3) Weighting parameters

Normally, the weight of each parameter is estimated based on the relative importance of the water quality parameter. Some WQI methods use experts to implement the parameter weighting process (Sarkar and Abbasi, 2006). Here, we also used the AHP method to determine WQI weights for the water quality parameters. Each of the experts determined the most appropriate weights for given parameters that reflect their influence on the overall water quality. All final weights were 0.24, 0.15, 0.20, 0.22, and 0.19 for the DO, T, TN, TOC, and TSS parameters, respectively.

(4) Aggregating WQI

A simple additive aggregation function was used to calculate the WQI value, which is given as follows:

$$z = \sum_{i=1}^{L} \omega_i S_i \tag{10}$$

where z is the WQI value; ω_i are weights of the individual indicators, which are derived by experts in the last step; and L is the total number of parameters.

After generating the WQI value, we retrieved the score values of the assessment results at the same 15 sampling sites from the raster overall

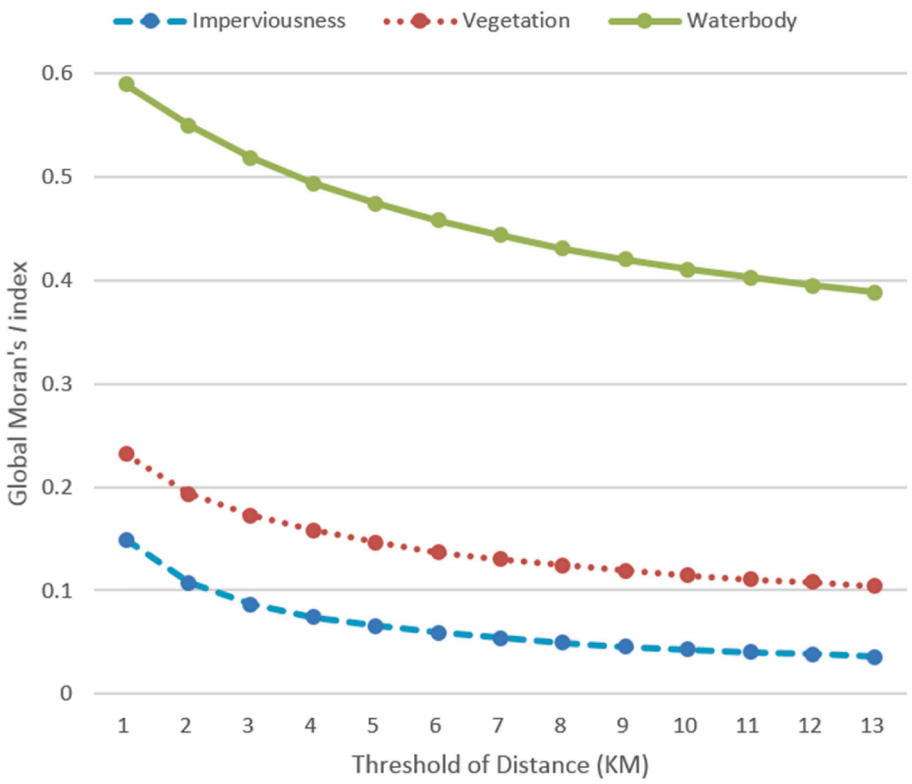

Fig. 3. Global Moran's *I* indexes for waterbodies, vegetation covers and imperviousness with different distance thresholds. When the distance thresholds increased, the global Moran's *I* indexes of all features decreased.

score map, which was generated by our method. Then, Pearson's correlation coefficients between the WQI values and score values of the assessment results were calculated. Thus, we used the WQI values of water quality to validate the overall score values of wetland conditions generated by our method.

4. Results

4.1. Ecological indicators and wetland condition mapping

4.1.1. Global Moran's I indexes

The global Moran's *I* indexes for waterbodies, vegetation covers and imperviousness were calculated using different distance thresholds. As shown in Fig. 3, the global Moran's *I* indexes of all features decreased, and the *p*-value was close to 0 when the distance threshold increased. For imperviousness and vegetation, the decreasing trend of the global Moran's *I* index became slow when the value of the distance threshold was >6 km. For waterbodies, their distribution and area were wider than those of imperviousness and vegetation coverage, so their global Moran's *I* index values were greater than those of imperviousness and vegetation coverage. When the value of the distance threshold was >10 km, the decreasing trend of the global Moran's *I* index of waterbodies became slow. That is, the optimal distances of spatial autocorrelations of waterbodies, vegetation covers and imperviousness were 10 km, 6 km and 6 km, respectively.

4.1.2. Density maps of indicators

The density maps of indicators were calculated using the kernel density tool in ArcGIS 10.3 (Fig. 4(a)–(e)). The value range of each indicator varies across the whole study area can be seen here.

4.1.3. Overall score mapping of wetland condition

Overall score mapping of wetland conditions, which covered the whole boundary of Suzhou, was implemented using the KBRM approach (Fig. 5). The value of the overall score map ranged from 15.6 to 82.9, the mean was 61.5, and the standard deviation was 9.2. In general, cells with higher values were found in urban regions, while cells with lower values were observed in lake or forest regions.

4.1.4. Correlation between KBRM output and ecological indicators

We calculated the correlation between the KBRM output and five indicators, which is given in Fig. 6. The KBRM output has a strong correlation with waterbodies and imperviousness, and their values of correlation are 0.85 and −0.87, respectively.

Among the five indicators, the correlation between waterbodies and imperviousness is strong, and the value of the correlation is −0.73. No other pair of indicators has such a strong correlation. This demonstrated that the selection of these indicators is reasonable. There is no heavy multicollinearity among these indicators.

4.2. Wetland assessment

4.2.1. Five-level output of assessment

Fig. 7. shows the five-level output of wetland conditions, which is generated by using the natural breaks (Jenks) algorithm. The proportions of bad, poor, moderate, good, and excellent cases are 3.7%, 25.0%, 34.6%, 21.9%, and 14.8%, respectively (Table 3). For Yangchenghu wetland (13), Taihu Lakeshore Wetland Park (26), and Chenghu wetland (27), most cells within them are classified as excellect level.

4.2.2. Numerical variations of individual wetlands

Numerical variations in individual wetlands are shown in Fig. 8. Based on the average value of each wetland, 9 wetlands fall within the excellent category, while 2 wetlands fit into the poor or bad category. The three wetlands with the highest average values (best condition) are the Manshan Island Wetland (22), Taihu Sanshandao Wetland Park (47), and East Taihu Lake Wetland (48), with scores of 82.5, 81.6 and 81.4, respectively. The three wetlands with the lowest (worst condition)

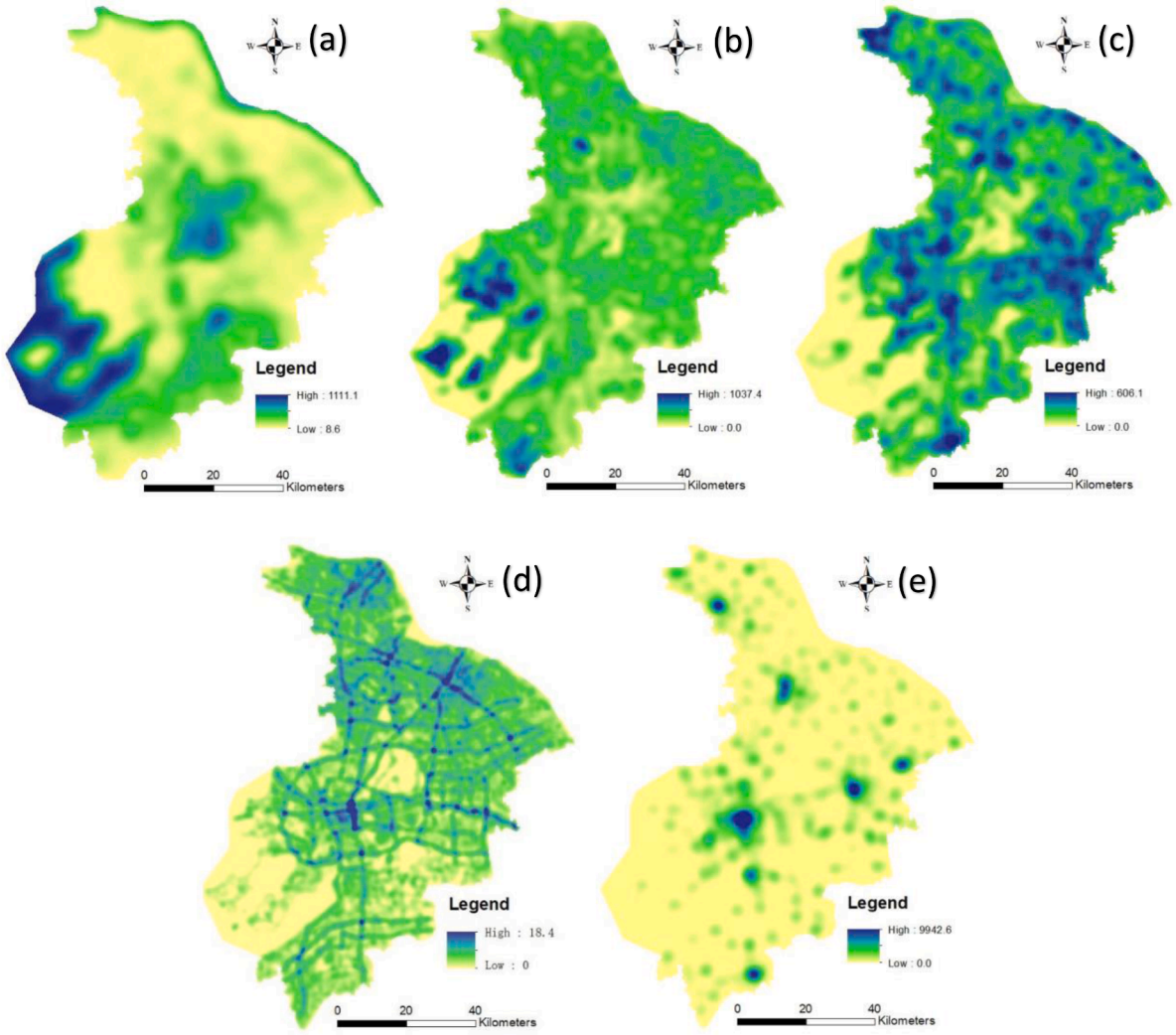

Fig. 4. Density maps of the ecological indicators calculated using the kernel density tool. (a) Density map of the waterbodies, (b) vegetation covers, (c) imperviousness, (d) roads, and (e) POI values.

average values are Xianzidou (58), Jiyang Lake Wetland Park (1), and Hetangyuese Wetland Park (17), with scores of 51.9, 53.6 and 57.7, respectively.

Additionally, the three wetlands with the highest std values of 3.9, 3.7, and 3.7 (i.e., South Yangchegnhu (15), Shanghu (3), and Kunchenghu (6)) are surrounded by various environmental types. The three wetlands with the lowest std values of 0.2 (i.e., Manshan Island Wetland (22), Zhangwandang Wetland Park (52), and Gongshan Island Wetland (16)) have little interior variation.

4.2.3. Spatial variations of overall wetlands

Spatial variations across all of the wetlands are shown in Fig. 9. The HH region is mostly located in the dense open water and vegetation region. This region has large lakes and forests and experiences slight human disturbance. Comparably, the LL region is mainly concentrated in dense urban regions. This region is affected by heavy human disturbance. Additionally, the HL region is mainly situated in hills surrounded by urban areas. The HL region is located in the transitional area of landscape types.

4.3. Validation

Pearson's correlation between the overall score values and WQI values of water quality is shown in Fig. 10. As we can see, Pearson's $r = 0.831$ at $p < 0.001$.

5. Discussion

We proposed a KBRM-based framework for wetland assessment. As a case study, we implemented this framework in the assessment of wetlands in Suzhou, China. The findings of this study can be summarized as follows:

The KBRM-based framework is an efficient and effective way to assess wetland ecological conditions. It is open and flexible to incorporating different types of data to adapt to different regions. It is good at encompassing the advantages of increasingly available remote sensing images (e.g., Landsat and Sentinel) and open social data (e.g., OSM and POI). In this way, it can be easily adapted to meet the needs of different management practices or different study areas. In particular, it is very useful when field sampling is expensive and wetland regions are large or inaccessible.

The lack of field data remained a challenge in wetland assessment in Suzhou. Zhu et al. (2019) developed a microbial community–based index of biotic integrity to evaluate the health of 15 wetland sites in Suzhou. Yang et al. (2016a) and Yang et al. (2016b) used landscape-scale indicators to carry out wetland assessments in the central urban region of Suzhou. In this study, for the first time, the entire administrative boundary of Suzhou was used as a study area, and the ecological

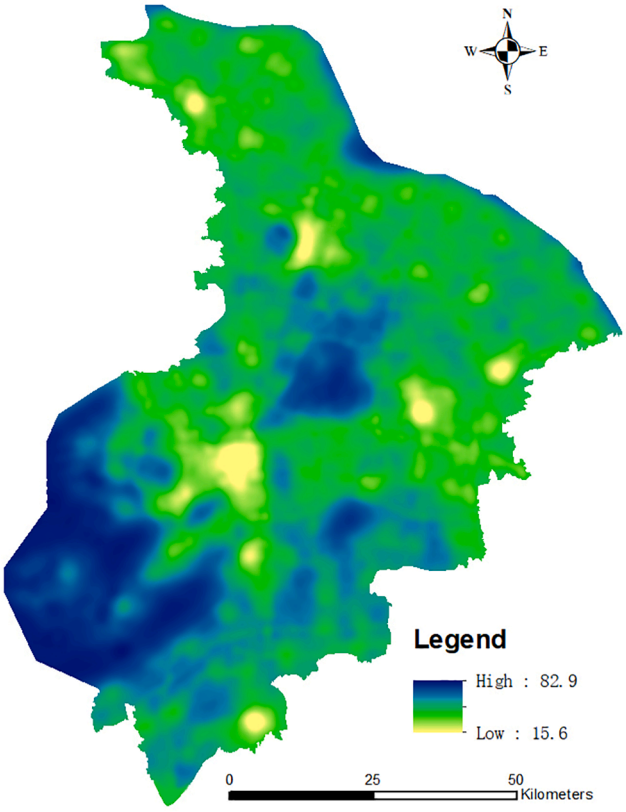

Fig. 5. Overall score mapping of wetland conditions generated using the KBRM approach.

conditions of 58 wetlands or wetland parks were assessed using remote sensing images and POI data.

Due to many ecological indicators potentially affecting wetland conditions, the dominant indicator of wetland conditions is still debatable. The results showed that a correlation exists between the KBRM output and each indicator. As expected, the density of waterbodies is a positive indicator, a higher value of which implies better wetland ecological conditions. The density of imperviousness, roads, and POI values are major negative indicators, which reflect poor wetland conditions when high. By combining positive and negative indicators, ecological integrity can be represented in the KBRM output. We find that the density of the waterbodies and density of imperviousness have the highest positive and negative correlations with the KBRM output. This result also highlights the importance of waterbodies and imperviousness as reliable indicators for wetland assessment, which was consistent with some earlier studies (Chen et al., 2019; Fernandez et al., 2019; Yang et al., 2016a). Additionally, the correlation between KBRM output and POI is −0.65, which indicates that POI can represent more details and obtain a finer scale effect on wetland conditions. However, the density of vegetation is a minor negative indicator in our study, which is inconsistent with our assumption and the results of other studies (Xu et al., 2018; Langan et al., 2019). This matter requires further research.

Considering that field measurements of wetlands in Suzhou are still limited, the ecological indicators for wetland assessment used in this framework have limitations. In the future, with the introduction of more spatial information technologies and data, more effective indicators will be introduced to improve the applicability and operability of this framework.

The ecological conditions of wetlands can be spatially distinguished and represented in detail. The natural breaks (Jenks) algorithm-based five-level output map makes the result more visually interpretable and meaningful in wetland assessment. Obvious numerical and spatial

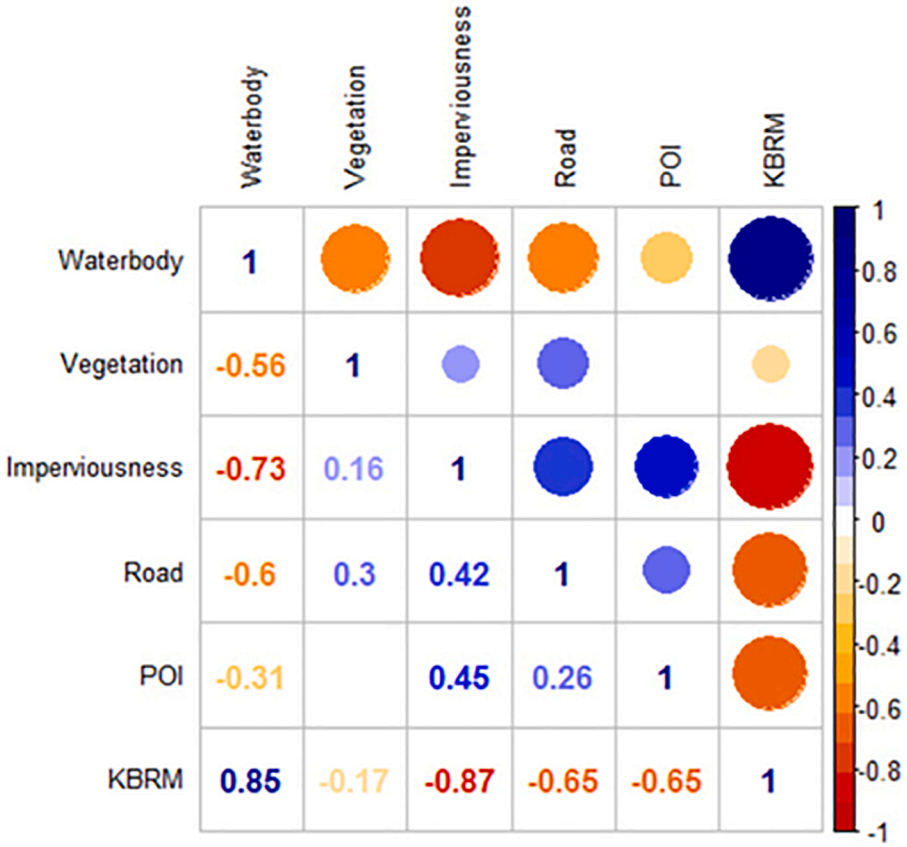

Fig. 6. Correlation analysis of the KBRM output and the five indicators.

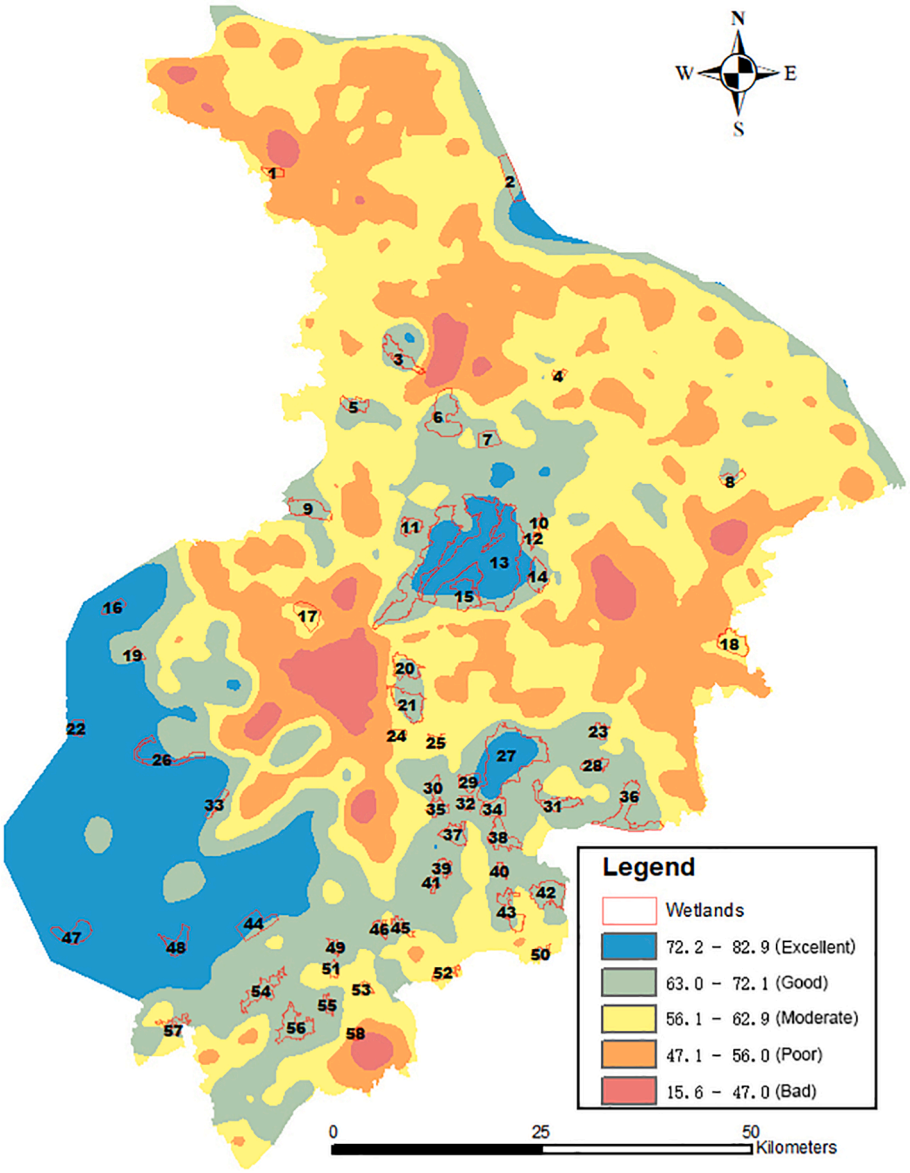

Fig. 7. Five-level output of assessment generated by the natural breaks (Jenks) algorithm and locations of validation points.

Table 3
Five levels of overall score map with value range, counts, area and area proportion.

Level	Value range	Counts	Area (km^2)	Area %
Excellent	72.2–82.9	1,194,683	1075.2	14.8
Good	63.0–72.1	1,760,258	1584.2	21.9
Moderate	56.1–62.9	2,788,412	2509.6	34.6
Poor	47.1–56.0	2,011,462	1810.3	25.0
Bad	15.6–47.0	296,047	266.4	3.7

variations in wetlands exist between the 58 wetlands in Suzhou. As expected, most of the wetlands with the best ecological conditions were located close to large lakes or far away from urban regions. For example, the Manshan Island Wetland (22), Taihu Sanshandao Wetland Park (47), and East Taihu Lake Wetland (48) have the best ecological conditions. They are not only relatively far away from urban areas but also surrounded by large open water areas. In contrast, most of the wetlands with the worst ecological conditions were closely associated with urban regions. They are facing severe problems, including strong human disturbances and vegetation degradation patterns. For example, the Xianzidou Wetland (58), Jiyang Lake Wetland Park (1), and Hetangyuese Wetland Park (17) exhibit the worst ecological conditions. They are all recreational wetland parks surrounded by large urban areas. This indicates that urbanization and open waterbodies were the main contributors to wetland conditions. This finding can be supported by other studies (Bastami, et al., 2015; Alyssa et al., 2013). In addition, the wetlands with the highest std values, which have great interior variation, are typically surrounded by various land cover and POI types. The

Table A1
The inventory of 58 wetlands in Suzhou with their assessment scores and area.

ID	Name	Counts	Area (km^2)	Min	Max	Mean	STD
1	Jiyang Lake Wetland Park	2466	2.219	48.0	57.3	53.6	2.3
2	Yangtze Riverside Wetland	8557	7.701	62.3	74.3	67.7	3.1
3	Shanghu	7487	6.738	50.0	70.0	66.5	3.7
4	Nicanglou Wetland Park	1389	1.250	56.6	61.7	58.8	1.4
5	South Lake Wetland Park	4688	4.219	60.8	66.6	64.8	1.4
6	Kunchenghu	15,659	14.093	53.4	72.1	68.3	3.7
7	Shajiabang Wetland Park	4651	4.186	63.5	66.8	65.6	0.7
8	Jincang Lake Wetland Park	3543	3.189	58.5	65.3	62.9	1.4
9	Caohu	9494	8.545	60.8	69.4	67.3	1.7
10	Bachenghu	1365	1.229	59.9	66.4	64.1	1.2
11	Shenzhedang	4256	3.830	64.7	70.9	69.1	1.4
12	Manlihu	1262	1.136	60.4	68.6	63.8	2.1
13	Yangchenghu	122,048	109.843	57.6	79.8	74.4	3.5
14	Kuileihu	7428	6.685	62.6	73.7	69.5	2.7
15	South Yangchegnhu	8509	7.658	62.3	77.8	72.1	3.9
16	Gongshan Island Wetland	3127	2.814	79.0	79.9	79.6	0.2
17	Hetangyuese Wetland Park	7758	6.982	52.1	60.9	57.7	2.3
18	Tianfu Wetland Park	8594	7.735	54.4	59.1	57.8	0.8
19	Taihu Lake Wetland Park	2560	2.304	67.8	72.1	70.1	1.1
20	Jingjihu	7528	6.775	58.2	66.8	63.8	2.0
21	Dushuhu	10,328	9.295	55.1	68.8	65.7	2.1
22	Manshan Island Wetland	3020	2.718	81.9	82.7	82.5	0.2
23	Shangyanghu	2427	2.184	63.1	66.5	65.7	0.7
24	Yinshanhu	1851	1.666	55.4	61.1	59.3	1.5
25	Huoditan	1878	1.690	58.8	61.7	60.8	0.6
26	Taihu Lakeshore Wetland Park	7897	7.107	68.8	80.4	76.0	3.2
27	Chenghu	44,176	39.758	64.4	78.1	74.1	2.4
28	Bailianhu	3240	2.916	64.7	68.4	67.5	0.9
29	Huangnidou	4471	4.024	64.5	73.8	70.1	2.0
30	Jiulihu	2536	2.282	66.0	68.1	67.3	0.5
31	Jinxi Wetland Park	7022	6.320	62.3	65.4	64.1	0.7
32	Muzhanghu	2399	2.159	64.6	69.7	67.2	1.2
33	Qixinlanyue Wetland Park	3196	2.876	68.5	75.0	72.5	1.3
34	Tongli Wetland Park	5695	5.126	65.6	72.2	69.6	1.3
35	Tonglihu	3363	3.027	59.6	67.7	65.8	1.5
36	Dianshanhu	14,530	13.077	61.9	70.5	67.7	2.0
37	Nanxinhu	5853	5.268	62.9	71.6	68.1	2.4
38	Baixianhu	8179	7.361	63.5	70.1	68.3	1.4
39	Shitoutan	3103	2.793	67.9	71.3	70.4	0.7
40	Sunjiadang	1302	1.172	64.7	67.8	66.4	0.8
41	Nanshenyang	1464	1.318	69.8	70.9	70.5	0.3
42	Yuandang	10,935	9.842	62.1	68.1	66.4	1.3
43	Sanbaidang	7200	6.480	59.3	66.6	64.0	1.8
44	Taihu oasis Wetland Park	10,085	9.077	67.9	79.0	74.4	2.9
45	Changqidang	1956	1.760	60.0	67.5	64.8	2.1
46	Zhangyadang	2300	2.070	61.1	66.4	64.9	1.1
47	Taihu Sanshandao Wetland Park	8408	7.567	80.6	82.3	81.6	0.5
48	East Taihu Lake Wetland	6192	5.573	76.9	82.9	81.4	1.4
49	Changdang	1683	1.515	64.5	67.8	66.4	0.8
50	Yuanlangdang	2055	1.850	61.1	63.6	63.0	0.5
51	Dalonghu	2222	2.000	60.3	66.6	63.8	1.7
52	Zhangwandang Wetland Park	2784	2.506	62.0	62.8	62.4	0.2
53	Yingdouhu	2215	1.994	56.5	61.6	58.6	1.1
54	Changyang	7813	7.032	65.5	70.8	69.2	1.3
55	Zhuangxiyang	1557	1.401	64.8	68.5	67.0	0.8
56	Beimayang	10,881	9.793	66.1	71.4	69.9	0.8
57	Jingyudang	4009	3.608	61.5	65.6	63.9	1.0
58	Xianzidou	1326	1.193	44.8	56.0	51.9	2.6

wetlands with the lowest std values, which have little interior variation, consist of simple land cover and POI types. This demonstrates that different parts of a wetland may be subject to a variety of stressors and influences, resulting in varying interior ecological conditions. This finding shows that our method not only provides an overall assessment of the entire wetland but also identifies interior variation within a certain wetland.

To validate the efficiency of the ecological condition assessment results, cross validation was conducted using the water quality assessment method, which is a detailed site-specific assessment method. We compared the overall score values and WQI values of water quality at 15 field sampling sites in Suzhou. The validation demonstrates that the results from the two methods are strongly correlated (Pearson's $r = 0.831$, $p < 0.001$). This result confirms that there is a strong correlation between our method and the WQI method. This means that the assessment result of our study is consistent with the water quality sampling result. This finding indicates that our method could provide a convenient and cost-effective approach to map and assess the ecological condition of wetlands.

Although our framework has the advantage of deriving and integrating various indicators from different kinds of original spatial data, some tasks still need to be achieved in future research. First, more useful expert knowledge could be derived and applied to our KBRM approach. According to expert knowledge, more appropriate indicators can be selected,

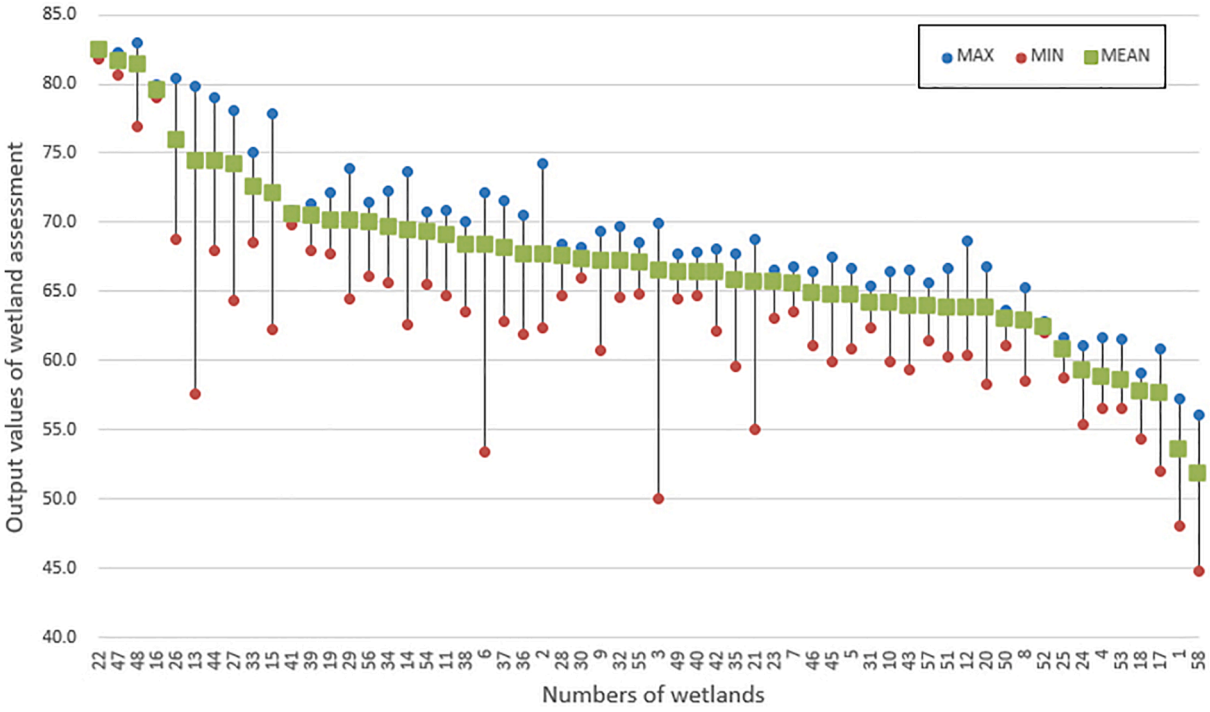

Fig. 8. Numerical variations of the 58 wetlands. Blue points, red points and green squares show the maximum, minimum, and average values of individual wetlands, respectively. (For interpretation of the references to colour in this figure legend, the reader is referred to the web version of this article.)

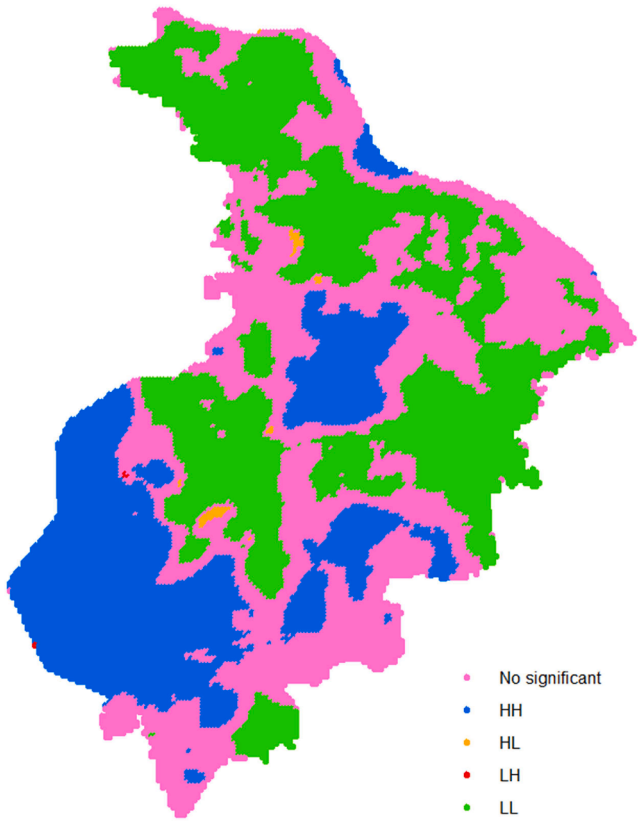

Fig. 9. Local Moran's I_i cluster map. HH indicates high values surrounded by high neighboring values; LL indicates low values surrounded by low neighboring values; LH indicates low values surrounded by high neighboring values; and HL indicates high values surrounded by low neighboring values.

and more suitable weights can be assigned to each indicator. This may improve the assessment accuracy of our study and extend this framework globally as well. Second, other than its applications to lacustrine wetlands, this KBRM approach needs to be widely implemented in other kinds of wetlands, such as swamp wetlands, to make it more generalized.

6. Conclusions

Based on remote sensing images and open social data, an easy and effective accessible framework for wetland assessment was developed. We proposed five indicators derived from open waterbodies, vegetation covers, imperviousness, road networks and POI values that were practical, cost-effective, and ecologically meaningful in measuring the ecological condition of wetlands. The KBRM approach was used to integrate these indicators and map ecological conditions. Our method has the advantage of convenient data collection, wide-region coverage, low cost, and spatial variation demonstration. It is not a substitute for the more detailed field assessment methods, but it can provide the opportunity to monitor and assess areas inaccessible by foot. In this way, it can be used to evaluate more wetlands than other field-based methods. Practitioners can easily use this framework to improve wetland research, restoration, and management.

The validation between our method and the water quality sampling method indicated that our method was reasonable and effective. It was possible to evaluate spatial variations in ecological conditions and provide solid support for policy-making in support of wetland protection and management. In the future, this method could be widely applied to different kinds of wetlands to make wetland protection and management more efficient and effective.

Declaration of Competing Interest

The authors declare that they have no known competing financial interests or personal relationships that could have appeared to influence the work reported in this paper.

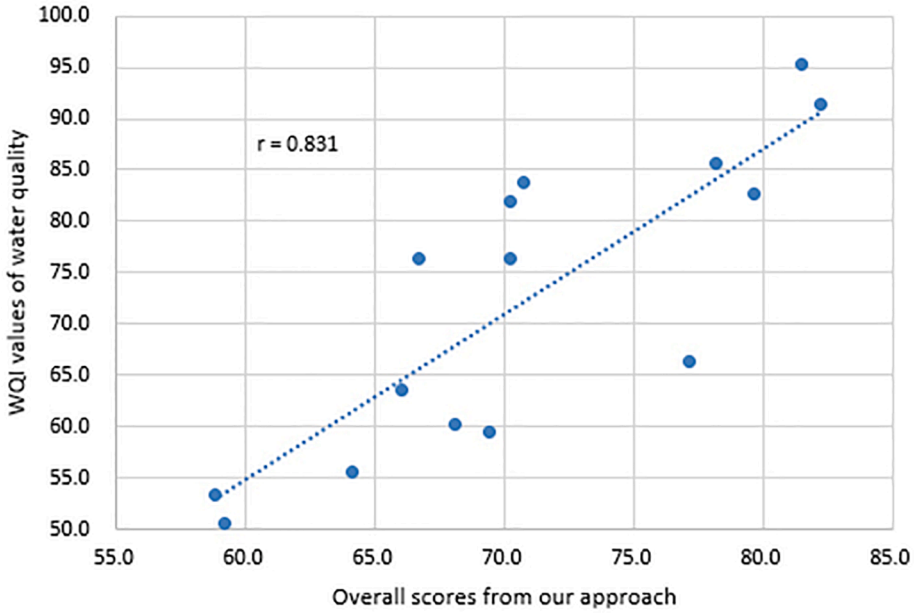

Fig. 10. Comparison between the overall scores of wetland conditions from our approach and the WQI values of water quality at 15 sampling sites. Pearson's correlation between them is 0.831 where $p < 0.001$. Generally, WQI values increase as the overall scores increase.

Acknowledgments

The authors thank the Wetland Protection Station of Suzhou for providing the data. This research is funded by the National Natural Science Foundation of China (Grant No. 41701477) and the Jiangsu Province Natural Science Foundation, China (Grant No. BK20170379).

References

Alyssa, M., Baxter, L., Laura, G., Johnson, T., 2013. Spatial differences in denitrification and bacterial community structure of streams, relationships with environmental conditions. Aquatic Sci. 75, 275–284.
Arnold, C., Gibbons, C., 1996. Impervious surface coverage: The emergence of a key environmental indicator. J. Am. Plan. Assoc. 62, 243–258.
Ausseil, A.-G.-E., Dymond, J.R., Shepherd, J.D., 2007. Rapid mapping and prioritisation of wetland sites in the Manawatu-Wanganui region, New Zealand. Environ. Manage. 39, 316–325.
Bastami, K.D., Neyestani, M.R., Shemirani, F., Soltani, F., Haghparast, S., 2015. Heavy metal pollution assessment in relation to sediment properties in the coastal sediments of the southern Caspian Sea. Mar. Pollut. Bull. 92, 237–243.
Brooks, R., Wardrop, D., Bishop, J., 2004. Assessing wetland condition on a watershed basis in the Mid-Atlantic region using synoptic land-cover maps. Environ. Monit. Assess. 94, 9–22.
Brown, M.T., Vivas, M.B., 2005. Landscape development intensity index. Environ. Monit. Assess. 101, 289–309.
Chen, T.-S., Lin, H.-J., 2013. Development of a framework for landscape assessment of Taiwanese wetlands. Ecol Indic. 25, 121–132.
Chen, W., Cao, C., Liu, D., Tian, R., Wu, C., Wang, Y., Qian, Y., Ma, G., Bao, D., 2019. An evaluating system for wetland ecological health: Case study on nineteen major wetlands in Beijing-Tianjin-Hebei region, China. Sci. Total Environ. 666, 1080–1088.
Chen, W., Huang, H., Dong, J., Zhang, Y., Tian, Y., Yang, Z., 2018. Social functional mapping of urban green space using remote sensing and social sensing data. ISPRS J. Photogramm. Remote Sens. 146, 436–452.
Agency, C.E.P., 2002. National Surface Water Environmental Quality Standards of China (GB3838-2002). China Standards Presss, Beijing (in Chinese).
Choi, J., Peters, M., Mueller, R.O., 2010. Correlational analysis of ordinal data: From Pearson's r to Bayesian polychoric correlation. Asia Pacific Educ. Rev. 11 (4), 459–466.
Cools, J., Johnston, R., Hattermann, F.F., Douven, W., Zsuffa, I., 2013. Tools for wetland management: Lessons learnt from a comparative assessment. Environ. Sci. Policy 34, 138–145.
Dobbie, M.J., Dail, D., 2013. Robustness and sensitivity of weighting and aggregation in constructing composite indices. Ecol. Indic. 29, 270–277.
EPA, U., 2006. Application of elements of a state water monitoring and assessment program for wetlands. Wetlands Division, Office of Wetlands, Oceans, and Watersheds, U.S. Environmental Protection Agency, Washington, DC.
Faber-Langendoen, D., Lemly, J., Nichols, W., Rocchio, J., Walz, K., Smyth, R., 2019. Development and evaluation of NatureServe's multi-metric ecological integrity assessment method for wetland ecosystems. Ecol. Indic. 104, 764–775.
Feng, L., Zhao, M., Zhou, Y., Zhu, L., Tian, H., 2020. The seasonal and annual impacts of landscape patterns on the urban thermal comfort using Landsat. Ecol. Indic. 110, 105798.
M. Fennessy A. Jacobs M. Kentula E. Control Review of rapid methods for assessing wetland condition 2004 Environmental Protection Agency Washington, D.C. EPA/620/R-04/009.
Fennessy, M.S., Jacobs, A.D., Kentula, M.E., 2007. An evaluation of rapid methods for assessing the ecological condition of wetlands. Wetlands 27, 543–560.
Fernandez, C., Spayd, J., Brooks, R.P., 2019. Landscape indicators and ecological condition for mapped wetlands in Pennsylvania, USA. Wetlands 39, 705–716.
Fox, D., 2014. Probability weighted indices for improved ecosystem report card scoring. Environmetrics 25, 351–360.
Goepel, K.D., 2013. Implementing the analytic hierarchy process as a standard method for multicriteria decision making in corporate enterprises – a new AHP excel template with multiple inputs. In: Proceedings of the International Symposium on the Analytic Hierarchy Process, pp. 1–10.
Hu, T., Yang, J., Li, X., Gong, P., 2016. Mapping urban land use by using landsat images and open social data. Remote Sens. 8, 151.
Huete, A.R., 1988. A soil-adjusted vegetation index (SAVI). Remote Sens. Environ. 25, 295–309.
Jenks, F., 1967. The data model concept in statistical mapping. Int. Yearbook Cartogr. 7, 186–190.
Jing, Y., Zhang, F., He, Y., Kung, H.-T., Johnson, V.C., Arikena, M., 2020. Assessment of spatial and temporal variation of ecological environment quality in Ebinur Lake Wetland National Nature Reserve, Xinjiang, China. Ecol. Indic. 110, 105874.
Lane, C.R., Brown, M.T., 2007. Diatoms as indicators of isolated herbaceous wetland condition in Florida, USA. Ecol. Indic. 7, 521–540.
Langan, C., Farmer, J., Rivington, M., Novo, P., Smith, J.U., 2019. A wetland ecosystem service assessment tool; Development and application in a tropical peatland in Uganda. Ecol. Indic. 103, 434–445.
Liu, C., Zhang, Q., Luo, H., Qi, S., Tao, S., Xu, H., Yao, Y., 2019a. An efficient approach to capture continuous impervious surface dynamics using spatial-temporal rules and dense Landsat time series stacks. Remote Sens. Environ. 229, 114–132.
Liu, X., He, J., Yao, Y., Zhang, J., Liang, H., Wang, H., Hong, Y., 2017. Classifying urban land use by integrating remote sensing and social media data. Int. J. Geograph. Inform. Sci. 31, 1675–1696.
Liu, Y., Li, T., Zhao, W., Wang, S., Fu, B., 2019b. Landscape functional zoning at a county level based on ecosystem services bundle: Methods comparison and management indication. J. Environ. Manage. 249, 109315.
Long, K., Wang, Y., Zhao, Y., Chen, L., 2015. Who are the stakeholders and how do they respond to a local government payments for ecosystem services program in a developed area: A case study from Suzhou, China. Habitat Int. 49, 1–9.
Mack, J.J., 2006. Landscape as a predictor of wetland condition: an evaluation of the Landscape Development Index (LDI) with a large reference wetland dataset from Ohio. Environ. Monit. Assess. 120, 221–241.
Mamoun, C.M., Nigel, R., Rughooputh, S.D.D.V., 2013. Wetlands' inventory, mapping and land cover index assessment on Mauritius. Wetlands 33, 585–595.
Mitsch, W.J., Gosselink, J.G., 2000. The value of wetlands: importance of scale and landscape setting. Ecol. Econ 35, 25–33.

Mollard, F., Foote, A., Wilson, M., Crisfield, V., Bayley, S., 2013. Monitoring and assessment of wetland condition using plant morphologic and physiologic indicators. Wetlands 33, 939–947.
Moran, P., 1948. The interpretation of statistical maps. J. Roy. Stat. Soc.: Ser. B (Methodol.) 10, 243–251.
Mwita, E., Menz, G., Misana, S., Becker, M., Kisanga, D., Boehme, B., 2013. Mapping small wetlands of Kenya and Tanzania using remote sensing techniques. Int. J. Appl. Earth Obs. Geoinf. 21, 173–183.
Pettorelli, N., Ryan, S., Mueller, T., Bunnefeld, N., Jedrzejewska, B., Lima, M., Kausrud, K., 2011. The normalized difference vegetation index (NDVI): unforeseen successes in animal ecology. Clim. Res. 46, 15–27.
Saaty, T., 1980. The analytic hierarchy process. McGraw-Hill, New York.
Salari, A., Zakaria, M., Nielsen, C.C., Boyce, M.S., 2014. Quantifying tropical wetlands using field surveys, spatial statistics and remote sensing. Wetlands 34, 565–574.
Sarkar, C., Abbasi, S.A., 2006. Qualidex – A new software for generating water quality indice. Environ. Monit. Assess. 119, 201–231.
Shi, X., Zhu, A., Burt, J., Qi, F., Simonson, D., 2004. A case-based reasoning approach to fuzzy soil mapping. Soil Sci. Soc. Am. J. 68, 885–894.
Shi, X., Long, R., Dekett, R., Philippe, J., 2009. Integrating different types of knowledge for digital soil mapping. Soil Sci. Soc. Am. J. 73, 1682–1692.
Silverman, B.W., 1986. Density estimation for statistics and data analysis. Chapman and Hall, New York.
Srebotnjak, T., Carr, G., de Sherbinin, A., Rickwood, C., 2012. A global Water Quality Index and hot-deck imputation of missing data. Ecol. Indic. 17, 108–119.
Stryszowska-Hill, K.M., Benson, C.E., Carberry, B., Twiss, M.R., Langen, T.A., 2019. Performance of wetland environmental quality assessment indicators at evaluating palustrine wetlands in northeastern New York State. Ecol. Indic. 98, 743–752.
Sun, T., Lin, W., Chen, G., Guo, P., Zeng, Y., 2016. Wetland ecosystem health assessment through integrating remote sensing and inventory data with an assessment model for the Hangzhou Bay, China. Sci. Total Environ. 566–567, 627–640.
Committee, S.M.A., 2010. Investigation report on wetland resources in Suzhou. Suzhou, Jiangsu.
Tiner, R.W., 2018. Chapter 2.1 - Introduction to landscape-level wetland assessment. In: Dorney, J., Savage, R., Tiner, R.W., Adamus, P. (Eds.), Wetland and Stream Rapid Assessments. Academic Press, pp. 9–18.
Tran, C., Vu, D., Shin, W., 2021. An improved approach for estimating social POI boundaries with textual attributes on social media. Knowledge-Based Systems 213,106710.
Tucker, C.J., Vanpraet, C.L., Sharman, M.J., Van Ittersum, G., 1985. Satellite remote sensing of total herbaceous biomass production in the senegalese sahel: 1980–1984. Remote Sens. Environ. 17, 233–249.
Uddin, M., Nash, S., Olber, T.A., 2021. A review of water quality index models and their use for assessing surface water quality. Ecol. Indic. 122, 107218.
Upton, G., Fingleton, B., 1985. Spatial data analysis by example, volume 1: point pattern and quantitative data. Wiley.
Wang, C., Wang, G., Guo, Z., Dai, L., Liu, H., Li, Y., Chen, H., Zhao, Y., Zhang, Y., Cheng, H., 2020. Effects of land-use change on the distribution of the wintering red-crowned crane (Grus japonensis) in the coastal area of northern Jiangsu Province, China. Land Use Policy 90, 104269.
Weller, D.E., Snyder, M.N., Whigham, D.F., Jacobs, A.D., Jordan, T.E., 2007. Landscape indicators of wetland condition in the Nanticoke River watershed, Maryland and Delaware, USA. Wetlands 27, 498–514.
Wilson, M.J., Bayley, S.E., 2012. Use of single versus multiple biotic communities as indicators of biological integrity in northern prairie wetlands. Ecol. Indic. 20, 187–195.
Xiao, X.D., Dong, L., Yan, H., Yang, N., Xiong, Y., 2018. The influence of the spatial characteristics of urban green space on the urban heat island effect in Suzhou Industrial Park. Sustain. Cit. Soc. 40, 428–439.
Xu, H., 2006. Modification of normalised difference water index (NDWI) to enhance open water features in remotely sensed imagery. Int. J. Remote Sens. 27, 3025–3033.
Xu, H., 2008. A new index for delineating built-up land features in satellite imagery. Int. J. Remote Sens. 29, 4269–4276.
Xu, H., Wang, M., Shi, T., Guan, H., Fang, C., Lin, Z., 2018. Prediction of ecological effects of potential population and impervious surface increases using a remote sensing based ecological index (RSEI). Ecol. Indic. 93, 730–740.
Yan, F., Liu, L., Li, Y., Zhang, Y., Chen, M., Xing, X., 2015. A dynamic water quality index model based on functional data analysis. Ecol. Indic. 57, 249–258.
Yang, Z., Shi, X., Su, Q., 2016a. Knowledge-based raster mapping approach to wetland assessment: A case study in Suzhou, China. Wetlands 36, 143–158.
Yang, Z., Feng, Y., Su, Qun, Qian, Xin, Chen, Z., Zhang, M., 2016b. Health assessment of wetlands in Suzhou using cellbased inverse-distance weighting landscape development intensity. Wetland Sci. Manage. 12, 16–20 (in Chinese).
Yang, Z., Su, Q., Chen, Z., Bai, J., Qian, X., 2017. Landscape health assessment for Sanshan Island of Tai Lake National Wetland Park in Suzhou. Wetland Sci. 15, 657–665 (in Chinese).
Zhu, W., Liu, Y., Wang, S., Yu, M., Qian, W., 2019. Development of microbial community–based index of biotic integrity to evaluate the wetland ecosystem health in Suzhou, China. Environ. Monit. Assess. 191, 377.